Electronic Supplementary Material (ESI) for New Journal of Chemistry.

Supporting information

A synergistic heterogeneous interface of a NC-Co-MoS_2/CC-450 electrocatalyst for efficient alkaline hydrogen evolution

Kaiqi zhang[a], Hequn Wu[a], Guanghui Xiong[a], Weifeng Yao[a, b, c]*

[a] Shanghai Key Laboratory of Materials Protection and Advanced Materials in Electric Power, College of Environmental & Chemical Engineering, Shanghai University of Electric Power, Shanghai, P. R. China.

[b] Shanghai Institute of Pollution Control and Ecological Security, Shanghai, PR China.

[c] Shanghai Engineering Research Center of Heat-exchange System and Energy Saving, Shanghai University of Electric Power, Shanghai, PR China

*Corresponding author E-mail address: yaoweifeng@shiep.edu.cn

Pretreatment of carbon cloth (CC)

The carbon cloth was cut into 2 cm × 4 cm and refluxed in a mixed solution of concentrated nitric acid/concentrated sulfuric acid (60 mL) with a volume ratio of 3:1 at 80 °C for 4 h to remove impurities on the surface of the carbon cloth and increase the hydrophilicity of the carbon cloth. After the solution was cooled to room temperature, the carbon cloth was removed and sonicated with acetone, ethanol, and deionized water for 10 min respectively, and then rinsed with deionized water to remove the residual acid on the surface of the carbon cloth. Finally, the carbon cloth was dried in a vacuum drying oven at 60 °C for 8 h, and then sealed and stored for use.

Preparation of ZIF67

First, 3 mmol $(Co(NO_3)_2 \cdot 6H_2O$ and 25 mL of methanol were added to a 100 mL A conical flask and mixed well with constant stirring. Next, 12 mmol of 2-methylimidazole and 25 mL of methanol were added to 100 mL of conical flask B and mixed with stirring to form a clear and transparent solution. Then the solution in the B conical flask was added to the A conical flask with constant stirring and stirred in a constant temperature water bath at 25 °C for 24 h. After stirring, the reaction products were collected by centrifugation and washed with methanol several times, and finally the products were placed in a vacuum drying oven at 60 °C for 12 h to obtain ZIF67, which was sealed and stored.

Preparation of $(NH_4)_2Mo_3S_{13} \cdot 2H_2O$

$(NH_4)_2Mo_3S_{13} \cdot 2H_2O$ was prepared according to the method reported by previous

researchers[1]. First, 40.0 g of sulfur powder and 120 mL of ammonium sulfide solution were added to a spherical flask and mixed well to form a polysulfide ammonium solution. Then 4.0 g of $(NH_4)_6Mo_7O_{24}\cdot 4H_2O$ was added to the above spherical flask and stirred thoroughly again. The reaction solution was heated in a condensing reflux device under an oil bath at 90 °C for 15 h with constant stirring. During the heating reaction, the dark red $(NH_4)_2Mo_3S_{13}\cdot 2H_2O$ will be formed and precipitated continuously. At the end of the heating reaction, the spherical flask is cooled in an ice water bath, then filtered and separated, and the product is washed with carbon disulfide several times to remove the excess sulfide. Finally, the product was dried in a vacuum oven at 60 °C for 12 h, and then sealed and stored for use.

Preparation of Pt/C/CC

A mixture of 5 mg of 20 wt.% Pt/C, 198 μL of deionized water, 792 μL of isopropanol and 10 μL of Nafion reagent were formulated and sonicated for 60 min to form a uniformly dispersed ink. The prepared ink was uniformly drop-coated onto the pretreated carbon cloth (1 cm × 2 cm) and dried to obtain a Pt/C catalyst loading of about 2 mg cm^{-2}.

Material characterization

The crystal structure of the materials was analyzed using a Bruker D8 model X-ray diffraction (XRD) instrument with a Cu target as the source of the radiation (wavelength 1.5418 Å). XRD scans ranged from 5 to 90 degrees at a rate of 5° min^{-1}. Scanning electron microscopy (SEM) as well as elemental mapping (EDS) analysis (Zeiss Gemini SEM 300) were used to observe surface morphology and composition

of the samples. Transmission electron microscopy (TEM) images and EDS maps were collected from a JEM-2100F model electron microscope equipped with an X-MaxN 800T IE250 energy spectrometer. x-ray photoelectron spectroscopy (XPS) was performed with a Scientific K-Alpha x-ray photoelectron spectrometer from Thermo, USA, using an Al-Kα excitation source (1486.6 eV), operating at 12 kV, to analyze the chemical valence of the elements on the surface of the sample.

Electrochemical measurements

The electrochemical experiments were carried out using a CHI660E workstation. All materials prepared in this experiment were tested using in a standard three-electrode system. The prepared electrocatalyst was used as the working electrode with a test area of 1 cm^2 , while the Hg/HgO electrode and the carbon rod were used as the reference and counter electrode, respectively. Before each test, the electrolyte solution of 1.0 M KOH (pH=14) was purged with argon gas for 30 min to remove the oxygen contained in the electrolyte solution, and all tests were performed at room temperature. The potential measured through the reference electrode Hg/HgO was converted to reversible hydrogen electrode potential (RHE) according to $E_{RHE} = E_{Hg/HgO} + 0.098 + 0.0591pH$[2]. To evaluate the HER activity of the catalyst under alkaline conditions, linear scanning voltammetry (LSV) curves were performed at a scan rate of 5 mV s^{-1} in 1.0 M KOH solution with an iR compensation of 90%. The Tafel plots were derived from their corresponding LSV curves according to the Tafel equation ($\eta = b \log j + a$, where b is the Tafel slope and j is the current density[3]). The charge transfer impedance (R_{ct}) of the catalyst was measured by electrochemical

impedance spectroscopy (EIS) in the frequency range of 10^5 Hz to 10^{-1} Hz, and R_{ct} was chosen to be tested at an overpotential of 150 mV. The bilayer capacitance (C_{dl}) of the catalyst was calculated from the cyclic voltammetric curve (CV) in the non-Faraday potential region at 0.07-0.17 V vs. RHE. CV measurements were performed at scan rates of 10 ~ 50 mV s^{-1} to calculate the double-layer capacitances (C_{dl}) of the prepared catalysts, which was used to evaluate the electrochemically active surface area (ECSA) of the prepared catalysts (ECSA $\approx$ C_{dl}/C_S, C_S = 0.04 mF cm^{-2})[4]. The Faraday efficiency (FE) of the electrocatalyst for hydrogen precipitation was tested by the drainage gas collection method with a test area of 1.0 cm^2. calculations were performed according to the Faraday efficiency formula[5]: FE= $(V/V_m)/[(I\times t)/(n\times F)]$, where V is the experimentally measured volume of hydrogen, V_m is the molar volume of the gas (24.5 L mol^{-1}) at room temperature (25 °C), I is the tested current of 50 mA, t is the tested time (3600 s), n=2, is the number of electron transfer for the hydrogen evolution reaction, and F is the Faraday constant of 96485.3 C mol^{-1}. The HER stability of the electrocatalyst in 1.0 M KOH solution was investigated using the chronopotentiometry (CP) method.

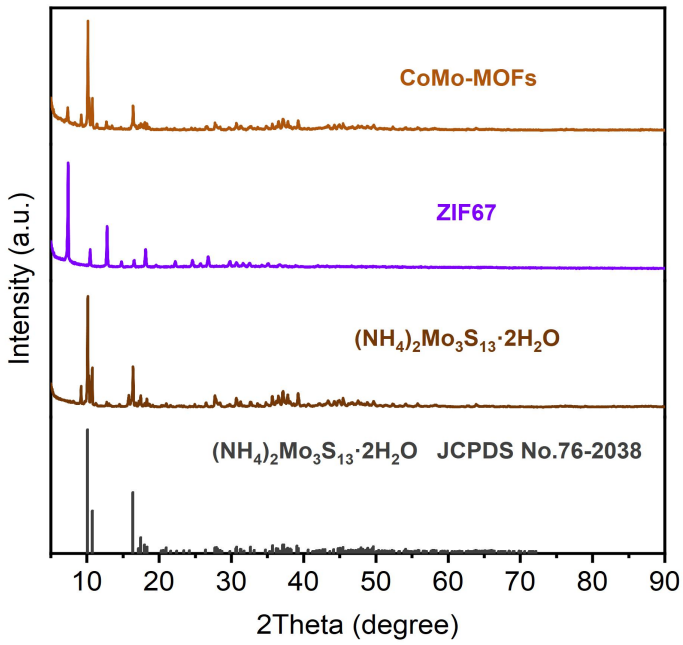

99

100 **Figure S1**. XRD patterns of CoMo-MOFs, ZIF67 and $(NH_4)_2Mo_3S_{13}\cdot 2H_2O$.

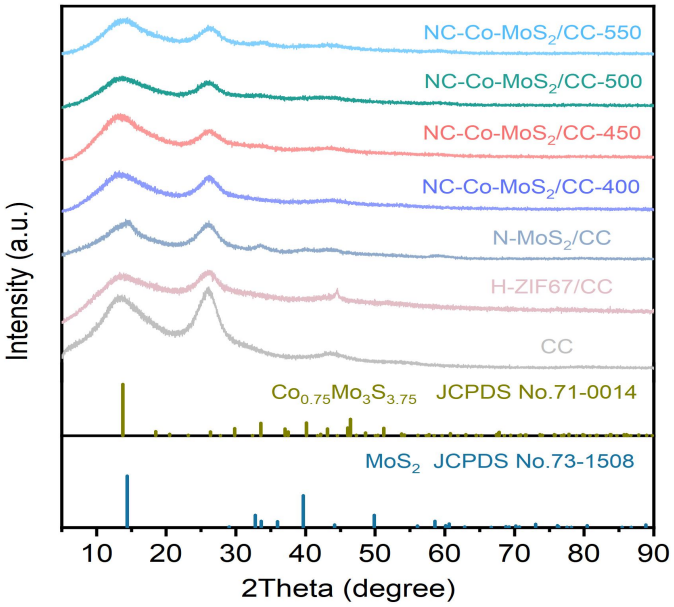

101

102 **Figure S2.** XRD patterns of NC-Co-MoS_2/CC-n (n=400, 450, 500 and 550),

103 N-MoS_2/CC, H-ZIF67/CC and carbon cloth (CC).

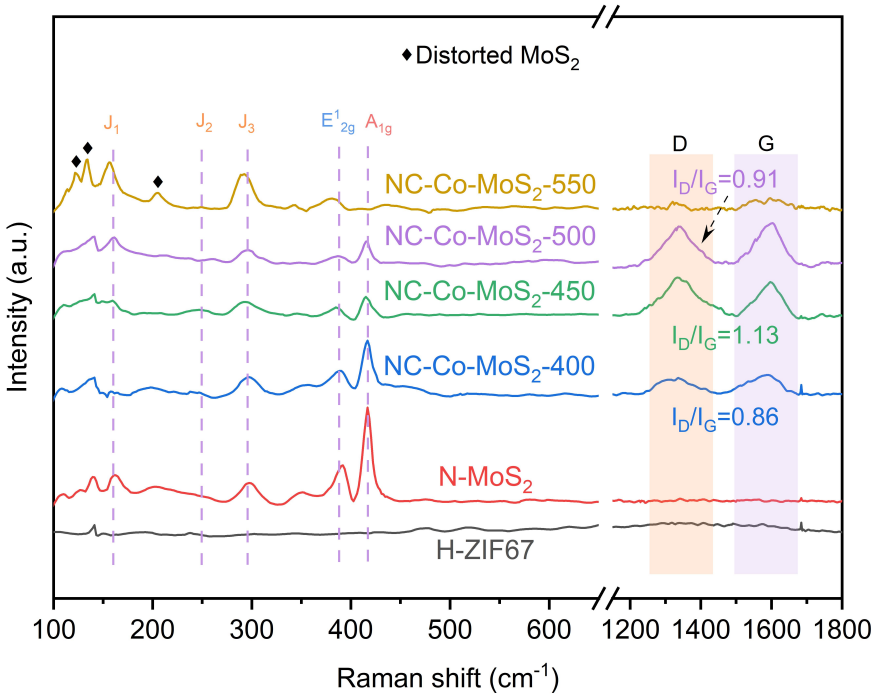

104

105 **Figure S3.** Raman patterns of NC-Co-MoS_2-n (n=400, 450, 500 and 550), N-MoS_2

106 and H-ZIF67.

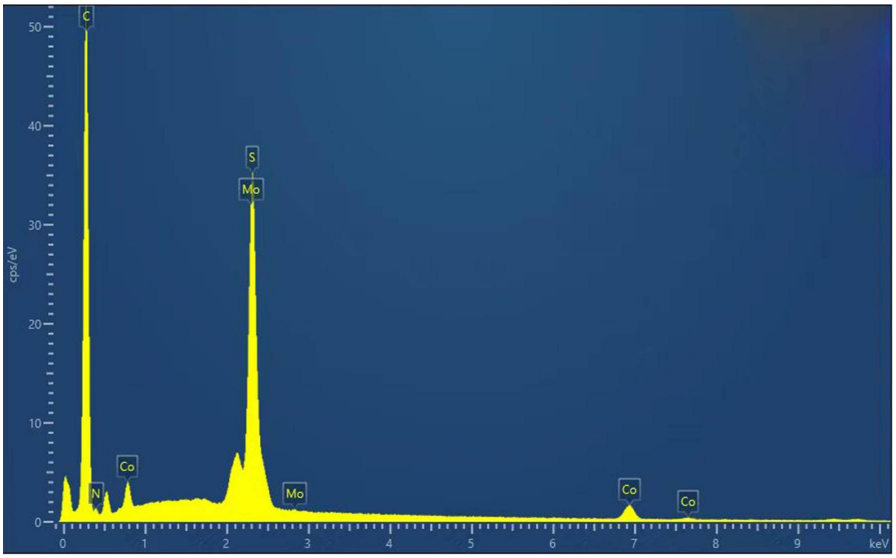

Figure S4. SEM EDS pattern of NC-Co-MoS_2/CC-450.

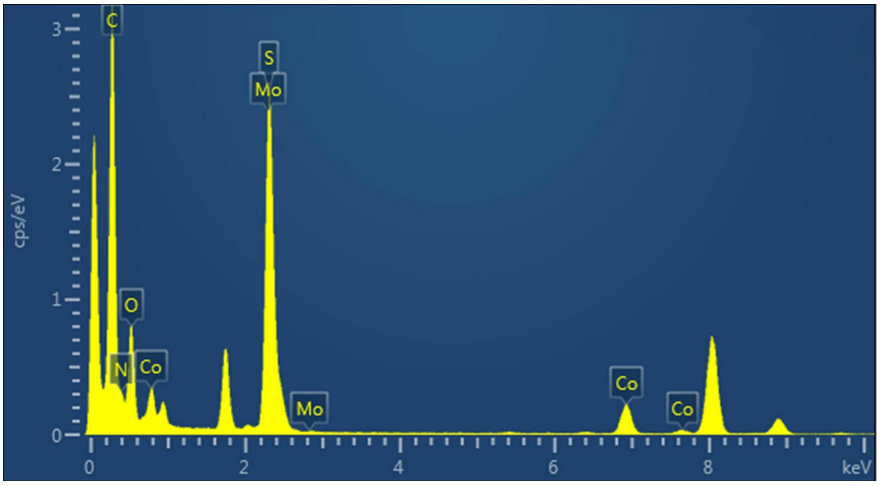

Figure S5. TEM EDS pattern of NC-Co-MoS_2/CC-450.

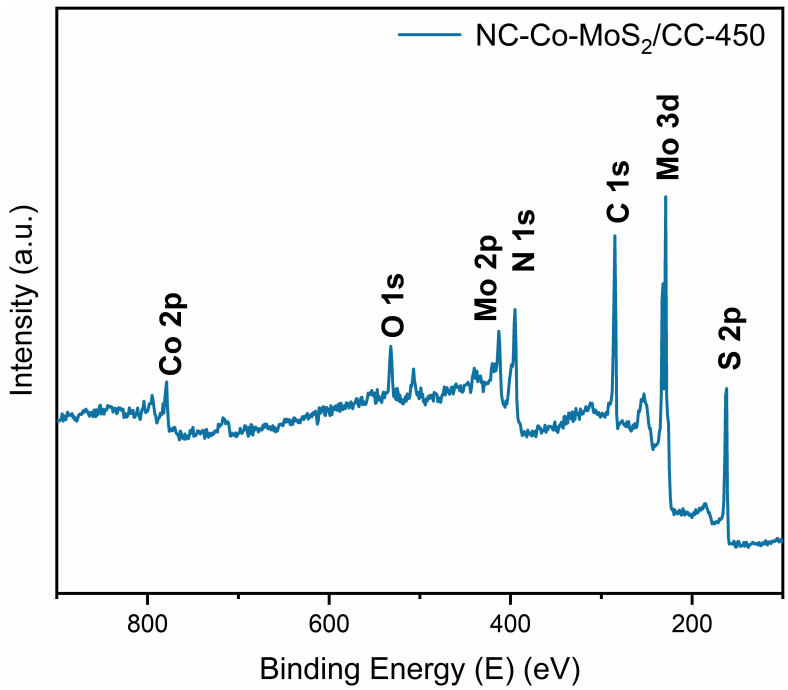

111

112 **Figure S6**. XPS surveys spectra of NC-Co-MoS_2/CC-450.

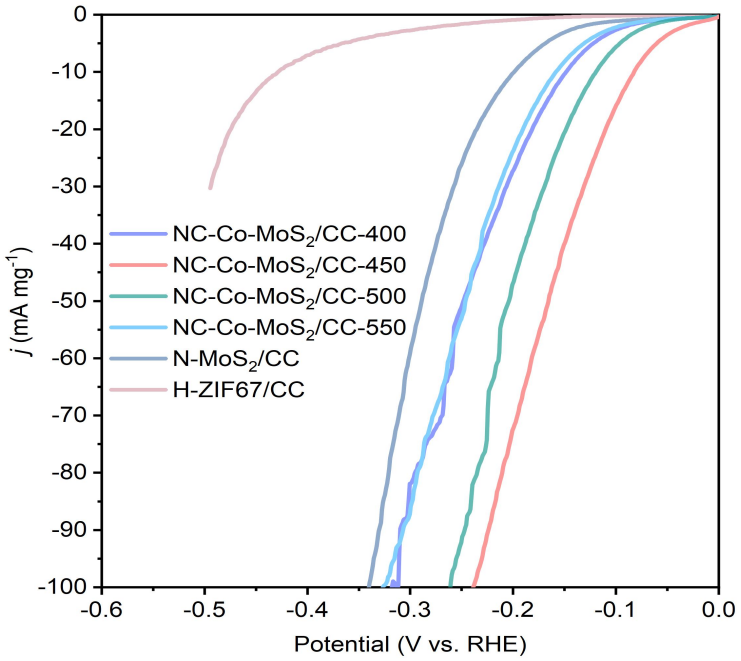

113

114 **Figure S7**. Loadings normalized current density curves for NC-Co-MoS_2/CC-n

115 (n=400, 450, 500 and 550), N-MoS_2/CC, H-ZIF67/CC catalysts

116

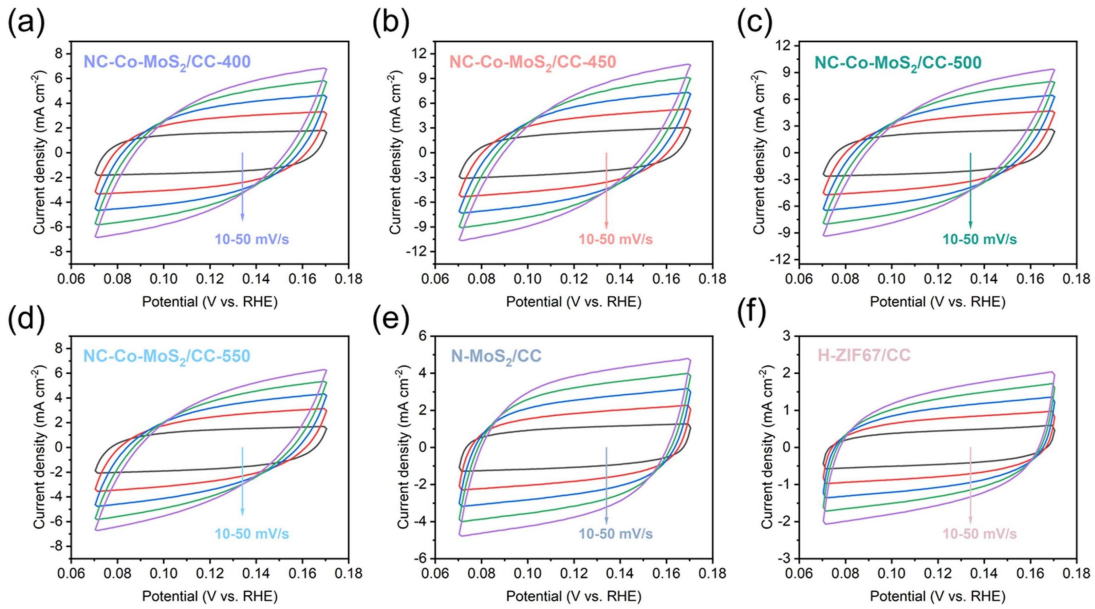

117

118 **Figure S8**. (a-d) Cyclic voltammograms of NC-Co-MoS_2/CC-n (n=400, 450, 500 and

119 550), (e) N-MoS_2/CC, (f) H-ZIF67/CC electrodes at 0.07-0.17 V vs. RHE.

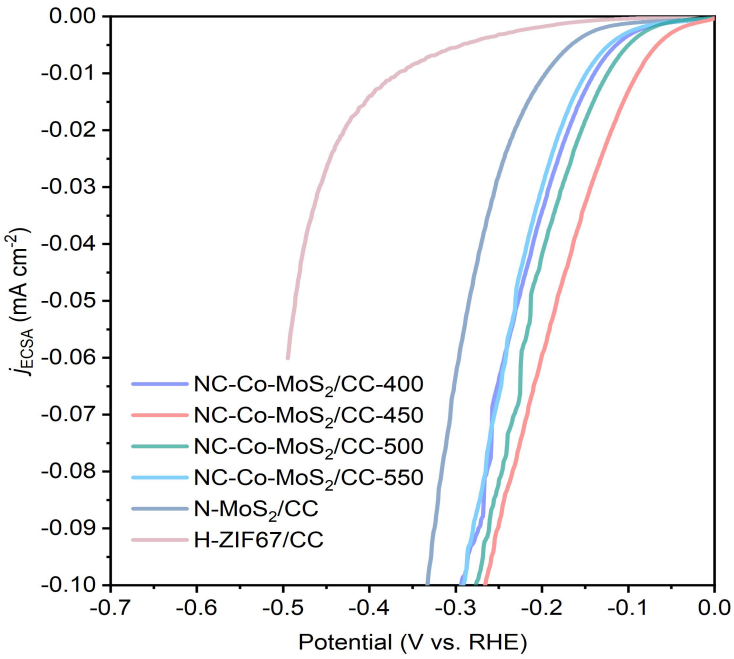

120

121 **Figure S9**. Electrochemical active area (ECSA) normalized current density curves for

122 NC-Co-MoS_2/CC-n (n=400, 450, 500 and 550), N-MoS_2/CC, H-ZIF67/CC catalysts.

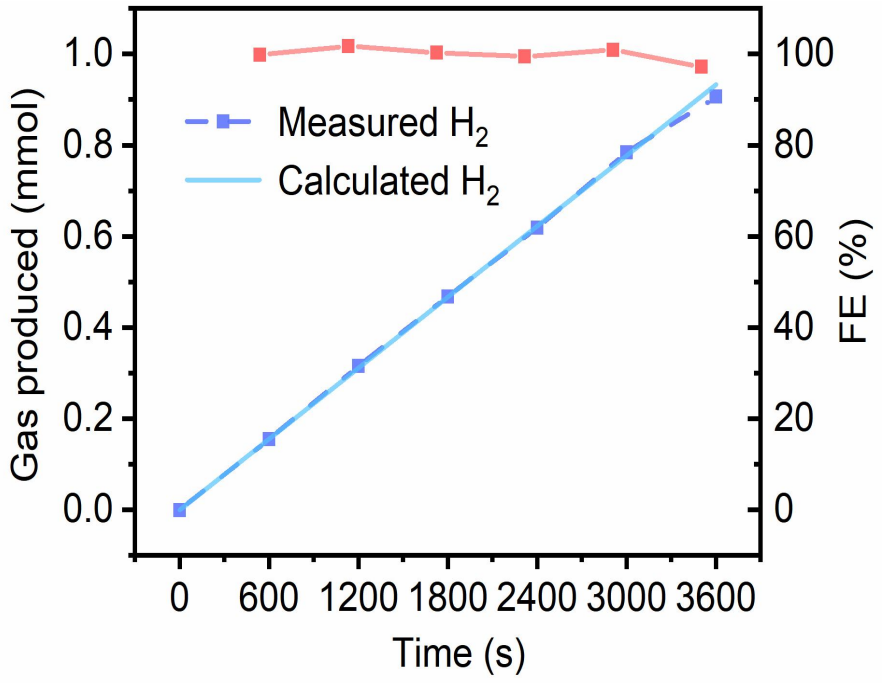

Figure S10. Hydrogen evolution Faraday efficiency plot for NC-Co-MoS_2/CC-450 electrocatalyst.

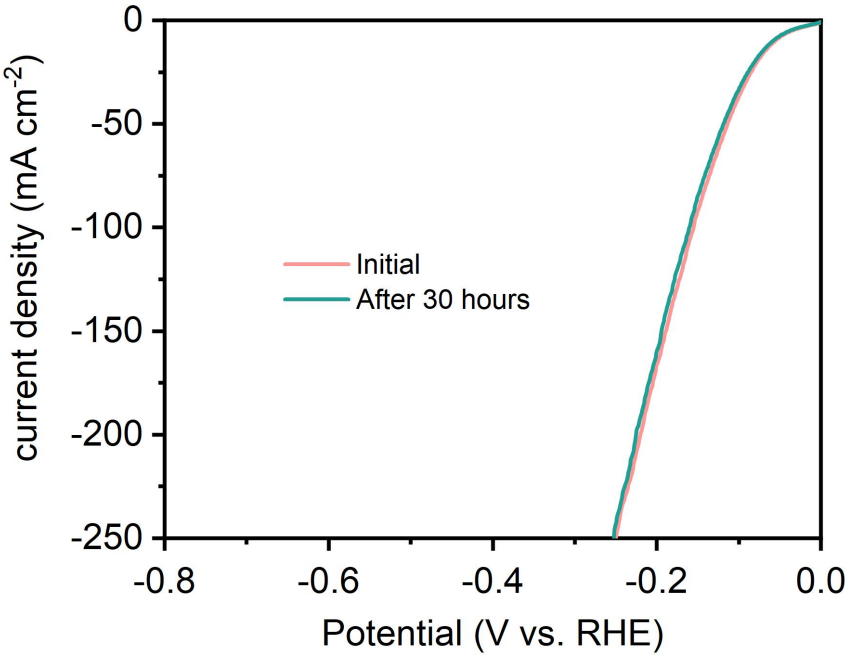

126

127 **Figure S11**. HER polarization curves of NC-Co-MoS_2/CC-450 electrocatalyst before

128 and after 30 h chronopotentiometry (CP) testing.

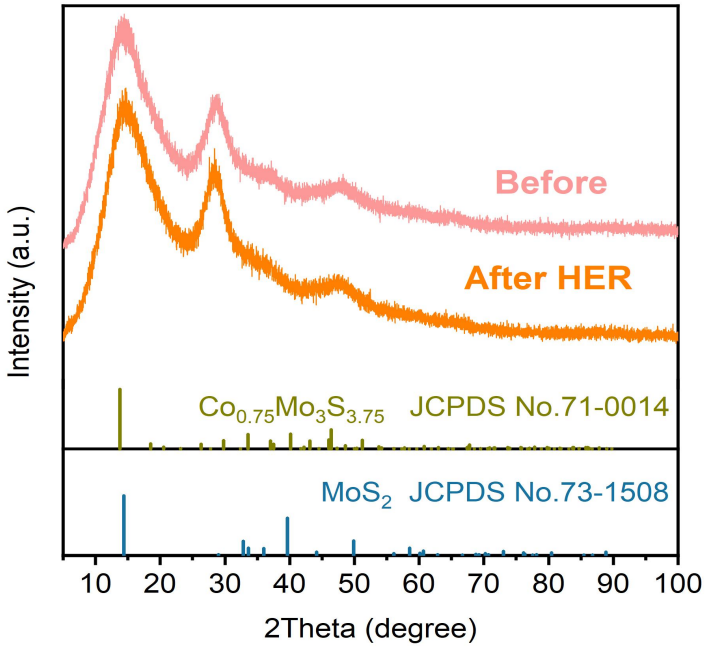

129

130 **Figure S12**. XRD patterns of NC-Co-MoS_2/CC-450 electrocatalyst before and after

131 30 h HER reaction chronopotentiometry (CP) testing.

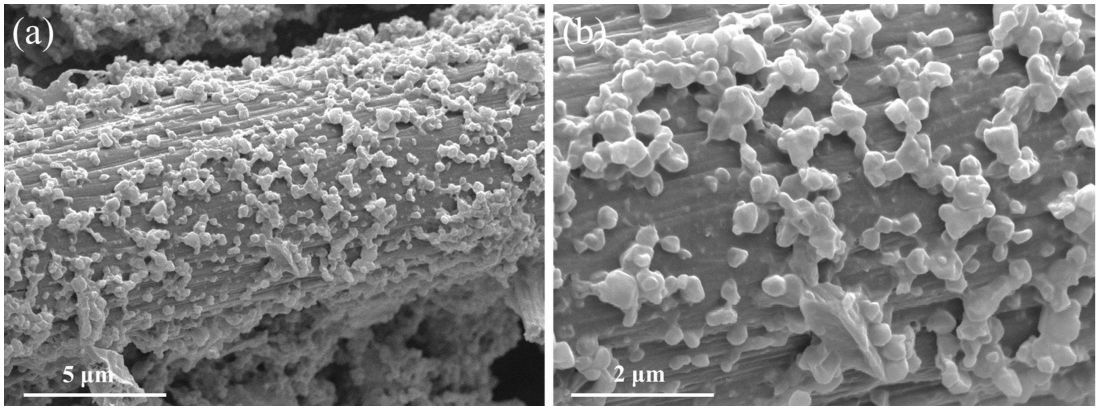

Figure S13. (a, b) SEM images of NC-Co-MoS_2/CC-450 electrocatalyst after HER chronopotentiometry (CP) stability testing.

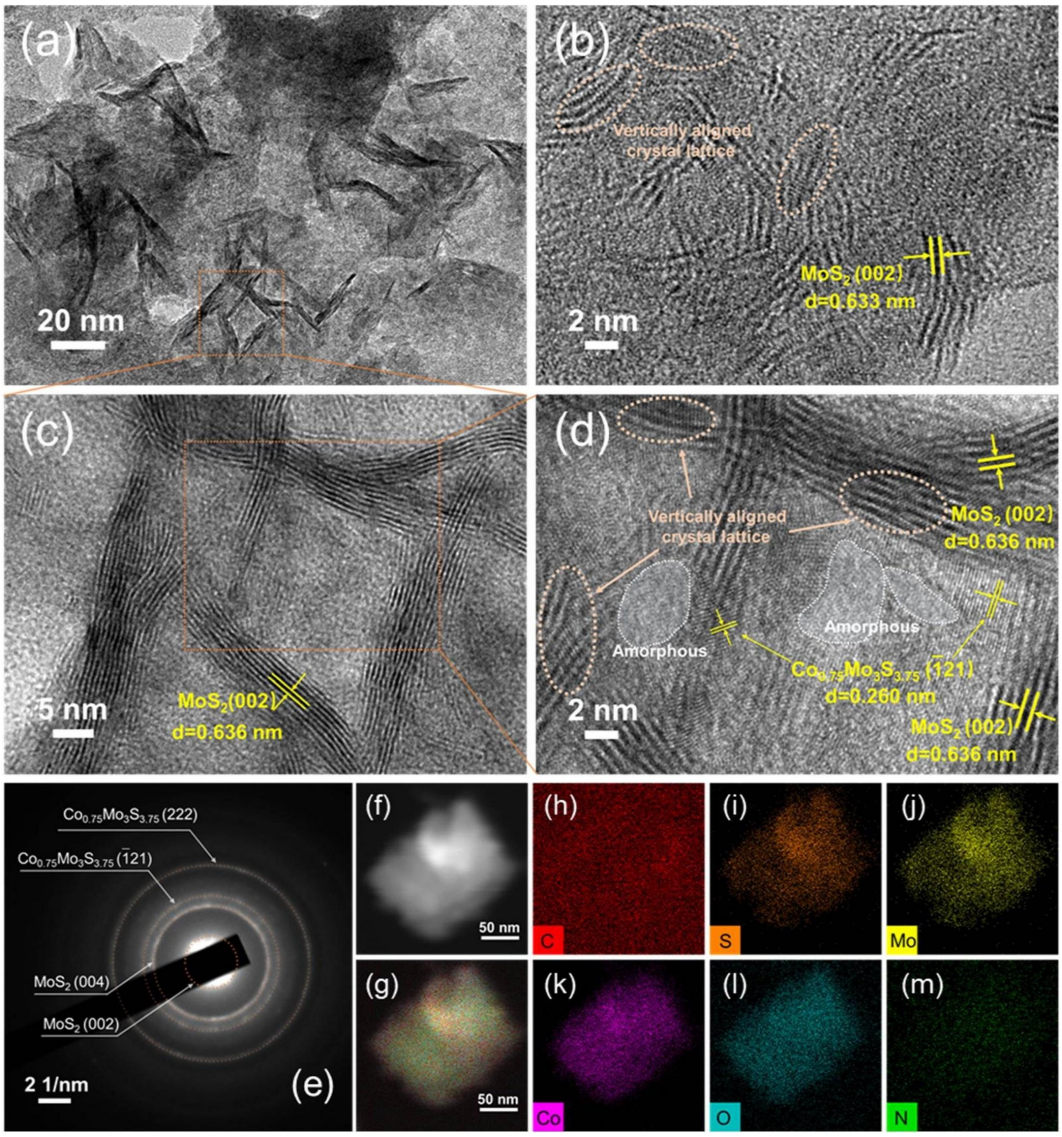

Figure S14. (a) TEM image; (b-e) HRTEM images and corresponding SAED images; (f-m) HAADF-STEM images and corresponding EDS mapping images of NC-Co-MoS_2/CC-450 catalyst after stability testing.

Table S1. The loadings of NC-Co-MoS_2/CC-n (n=400, 450, 500 and 550), N-MoS_2/CC, H-ZIF67/CC catalysts.

Catalyst	Initial Bare carbon cloth	After annealing	Mass loading (mg cm^{-2})
NC-Co-MoS_2/CC-400	0.0972 g	0.1164 g	2.40
NC-Co-MoS_2/CC-450	0.0980 g	0.1164 g	2.30
NC-Co-MoS_2/CC-500	0.0993 g	0.1167 g	2.18
NC-Co-MoS_2/CC-550	0.0986 g	0.1148 g	2.03
N-MoS_2/CC	0.0978 g	0.1124 g	1.83
H-ZIF67/CC	0.0985 g	0.1093 g	1.35

Table S2. Elemental content corresponding to the elemental mapping for the SEM of NC-Co-MoS_2/CC-450.

Element	Wt%	Atomic percentage
C	75.76	87.77
S	7.39	3.21
Mo	5.03	0.73
Co	4.01	0.95
O	3.29	2.86
N	4.52	4.49

Table S3. Elemental content corresponding to the elemental mapping for the TEM of NC-Co-MoS_2/CC-450

Element	Wt%	Atomic percentage
C	53.41	78.86
S	14.08	7.72
Mo	21.02	3.85
Co	3.62	1.08
O	6.62	7.28
N	1.25	1.21

Table S4. C_{dl} and ECSA values of NC-Co-MoS_2/CC-n (n=400, 450, 500 and 550), N-MoS_2/CC, H-ZIF67/CC catalysts

Catalyst	C_{dl} (mF cm^{-2})	ECSA (cm^2)
NC-Co-MoS_2/CC-400	76.38	1909.5
NC-Co-MoS_2/CC-450	111.76	2794
NC-Co-MoS_2/CC-500	97.62	2440.5
NC-Co-MoS_2/CC-550	64.35	1608.75
N-MoS_2/CC	68.27	1706.75
H-ZIF67/CC	27.22	680.5

Table S5. Comparison of the HER performances for NC-Co-MoS_2/CC-450 with reported electrocatalysts in 1.0 M KOH

Catalyst	**η(mV) @ *j* = 10,50,100 (mA cm^{-2})**	**Tafel slope (mV dec^{-1})**	**Current collector**	**Reference**
NC-Co-MoS_2/CC-450	η_{10} = 56 η_{50} = 114 η_{100} = 155	69.2	carbon cloth	This work
MoS_2/CoS_2	η_{10} = 67	70	carbon cloth	ACS Applied Energy Materials 2023, 6, 2479-2488[6]
CoS_2/MoS_2/NC	η_{10} = 215	80	GCE	Journal of Alloys and Compounds 2022, 891, 161962[7]
1T-Fe/P-WS_2@CC	η_{10} = 116	65	carbon cloth	Appl. Catal. B-Environ. 2021, 286, 119897[8]
1T-2H MoS_2/CoS_2	η_{10} = 37	46	carbon cloth	J. Mater. Chem. A 2022, 10, 16115-16126[9]
Co_9S_8-MoS_2/NF	η_{10} = 167	81.7	Nickel foam	Adv. Funct. Mater. 2020, 30, 2002536[10]
CoS_2-MoS_2	η_{10} = 130	66.8	GCE	Applied Surface Science 2020, 527, 146847[11]
Ni_3S_2@MoS_2/FeOOH	η_{10} = 95	49	Nickel foam	Appl. Catal. B-Environ. 2019, 244, 1004-1012[12]
CoS_2/MoS_2/RGO	η_{10} = 160	56	GCE	Applied Surface Science 2017, 412, 138-145[13]
N-MoS_2/CN	η_{10} = 114	46.8	GEC	J Am Chem Soc 2019, 141, 18578-18584[14]
MXene-MoS_2	η_{10} = 69	53	GCE	Nano Research 2023[15]
CC/MOF-$CoSe_2$@$MoSe_2$	η_{10} = 69	68.91	carbon cloth	Chemical Engineering Journal 2022, 429, 132379[16]
CoS_2/MoS_2-3	η_{10} = 163	63	GCE	ChemistrySelect 2022, 7, e202202700[17]
Ni_{SA}-MoS_2	η_{10} = 98	75	carbon cloth	Nano Energy 2018, 53, 458-467[18]

C+MoS_2@NF	η_{10} = 120	41.8	Nickel foam	Adv. Funct. Mater. 2023, 2214085[19]

157
158
159

References

1. A. W. Müller, V.; Krickemeyer, E.; Bögge, H.; Lemke, M., *Z. Anorg. Allg. Chem.*, 1991, **601**, 175-188.
2. S. Wang, P. Yang, X. Sun, H. Xing, J. Hu, P. Chen, Z. Cui, W. Zhu and Z. Ma, *Appl. Catal. B-Environ.*, 2021, **297**, 120386.
3. Y. Wang, G. Qian, Q. Xu, H. Zhang, F. Shen, L. Luo and S. Yin, *Appl. Catal. B-Environ.*, 2021, **286**, 119881.
4. X. Yin, R. Cai, X. Dai, F. Nie, Y. Gan, Y. Ye, Z. Ren, Y. Liu, B. Wu, Y. Cao and X. Zhang, *J. Mater. Chem. A*, 2022, **10**, 11386-11393.
5. H. Wen, L. Y. Gan, H. B. Dai, X. P. Wen, L. S. Wu, H. Wu and P. Wang, *Appl. Catal. B-Environ.*, 2019, **241**, 292-298.
6. Y. Zhu, J. Yao, L. Bai, W. Zhang, W. Wang, X. Ma and L. Wu, *ACS Appl. Energy Mater.*, 2023, **6**, 2479-2488.
7. K. Ji, K. Matras-Postolek, R. Shi, L. Chen, Q. Che, J. Wang, Y. Yue and P. Yang, *J. Alloys Compd.*, 2022, **891**, 161962.
8. D. R. Paudel, U. N. Pan, T. I. Singh, C. C. Gudal, N. H. Kim and J. H. Lee, *Appl. Catal. B-Environ.*, 2021, **286**, 119897.
9. P. Chang, T. Wang, Z. Liu, X. Wang, J. Zhang, H. Xiao, L. Guan and J. Tao, *J. Mater. Chem. A*, 2022, **10**, 16115-16126.
10. M. Kim, M. A. R. Anjum, M. Choi, H. Y. Jeong, S. H. Choi, N. Park and J. S. Lee, *Adv. Funct. Mater.*, 2020, **30**, 2002536.
11. Y. Zhou, W. Zhang, M. Zhang, X. Shen, Z. Zhang, X. Meng, X. Shen, X. Zeng and M. Zhou, *Appl. Surf. Sci.*, 2020, **527**, 146847.

12. M. Zheng, K. Guo, W. J. Jiang, T. Tang, X. Wang, P. Zhou, J. Du, Y. Zhao, C. Xu and J.-S. Hu, *Appl. Catal. B-Environ.*, 2019, **244**, 1004-1012.
13. Y. R. Liu, X. Shang, W. K. Gao, B. Dong, J. Q. Chi, X. Li, K. L. Yan, Y. M. Chai, Y. Q. Liu and C. G. Liu, *Appl. Surf. Sci.*, 2017, **412**, 138-145.
14. H. Wang, X. Xiao, S. Liu, C. L. Chiang, X. Kuai, C. K. Peng, Y. C. Lin, X. Meng, J. Zhao, J. Choi, Y. G. Lin, J. M. Lee and L. Gao, *J. Am. Chem. Soc.*, 2019, **141**, 18578-18584.
15. R. Zhang, Y. Sun, F. Jiao, L. Li, D. Geng and W. Hu, *Nano Res.*, 2023, DOI: 10.1007/s12274-023-5602-5.
16. S. J. Patil, N. R. Chodankar, S. K. Hwang, P. A. Shinde, G. Seeta Rama Raju, K. Shanmugam Ranjith, Y. S. Huh and Y.-K. Han, *Chem. Eng. J.*, 2022, **429**, 132379.
17. J. Xiong, Z. Cao, H. Wang, D. Ban, Z. Zhou, Y. Li and S. Chen, *ChemistrySelect*, 2022, **7**, e202202700
18. Q. Wang, Z. L. Zhao, S. Dong, D. He, M. J. Lawrence, S. Han, C. Cai, S. Xiang, P. Rodriguez, B. Xiang, Z. Wang, Y. Liang and M. Gu, *Nano Energy*, 2018, **53**, 458-467.
19. B. Gao, Y. Zhao, X. Du, D. Qian, S. Ding, C. Xiao, J. Wang, Z. Song and H. W. Jang, *Adv. Funct. Mater.*, 2023, DOI: 10.1002/adfm.202214085, 2214085.